1   **Title:** Immune Response Drives Outcomes in Prostate Cancer: Implications for

2   Immunotherapy

3   **Running title:** Prognostic Value of Immunophenotype in Prostate Cancer

4   Jialin Meng[1], Yujie Zhou[2], Xiaofan Lu[3], Zichen Bian[1], Yiding Chen[1], Song Fan[1], Jun Zhou[1], Li

5   Zhang[1], Zongyao Hao[1], Meng Zhang[1,4*], Chaozhao Liang[1*]

6   1. Department of Urology, The First Affiliated Hospital of Anhui Medical University; Institute of

7   Urology & Anhui Province Key Laboratory of Genitourinary Diseases, Anhui Medical

8   University, Hefei, 230022, P.R. China.

9   2. Division of Gastroenterology and Hepatology, Key Laboratory of Gastroenterology and

10   Hepatology, Ministry of Health, Renji Hospital, School of Medicine, Shanghai Jiao Tong

11   University, Shanghai Institute of Digestive Disease, Shanghai, 200127, P.R. China.

12   3. State Key Laboratory of Natural Medicines, Research Center of Biostatistics and

13   Computational Pharmacy, China Pharmaceutical University, Nanjing 211198, P.R. China.

14   4. Urology Institute of Shenzhen University, The Third Affiliated Hospital of Shenzhen

15   University, Shenzhen University, Shenzhen, 518000, P.R. China.

16   ***Correspondence to** Meng Zhang (zhangmeng1930@126.com) & Chaozhao Liang

17   (liang_chaozhao@ahmu.edu.cn).

18   **Tel.:** +8655162922234, and **Fax.:** +8655162922234

19   **Address:** Jixi Road 218, Shushan District, Hefei City 230022, Anhui Province, People's

20   Republic of China.

21

22

23 **Abstract**

24 **Background:** The heterogeneity of the immune microenvironment leads to the

25 different response results of immune checkpoint blockade therapy. We aimed to

26 propose a robust molecular classification of prostate cancer microenvironment to

27 identify ideal patients for delivering effective immunotherapy.

28 **Methods:** A total of 1,557 prostate cancer patients were enrolled in the current

29 study, including 69 real-world samples from the AHMU-PC cohort. Non-negative

30 matrix factorization algorithm was employed to virtually microdissect the patients

31 to immune and non-immune subclasses. The patients in the immune class were

32 dichotomized to immune activated and suppressed subtypes by the nearest

33 template prediction of activated stroma signature. The curative effects of different

34 immune subclasses in response to immunotherapy were also predicted.

35 **Results:** We termed the newly identified molecular class of tumors as "immune

36 class", which was characterized by a high enrichment of T cell, B cell, NK cell,

37 macrophage associated signatures, *etc.*, compared with the non-immune class (all,

38 $P < 0.05$). Subsequently, the immune class was subclassified into immune

39 activated and suppressed subtypes determined by the activation status of

40 WNT/TGF-β, TGF-β1, and C-ECM signatures. As a result, around 14.9% to 24.3%

41 of overall patients belonged to the immune activated subgroup, and they were

42 proved with the favorable recurrence-free survival outcomes than others and

43 showed potential curative effects in response to the anti-PD-1/PD-L1

44 immunotherapy.

2

45 **Conclusion:** Our study identifies a novel immune class in prostate cancer, which

46 is further described by active or exhausted immune responses. These findings

47 provide novel insights into tailoring immunotherapeutic strategies for different

48 prostate cancer subgroups.

49 **Keywords:** Prostate cancer, tumor immune microenvironment, immune molecular

50 subgroups, non-negative matrix factorization, immunotherapy, PD-L1, immune

51 checkpoint blockade

52 **Highlights**

53 ■ Immunotherapy could trigger a durable response in advanced prostate cancer,

54   but it only benefits a minority of patients;

55 ■ Immune response drives recurrence-free survival outcomes in prostate cancer;

56 ■ The robust molecular classification system helps identify more ideal patients

57   for delivering anti-PD-1/PD-L1 immunotherapy.

58 **Introduction**

59 Since the prostate cancer ranks as the second most frequent tumor and leads to

60 the fifth tumor-specific death among males, the substantial burden of prostate

61 cancer around the world attracts amounts of health concerns [1]. The outcomes of

62 low-intermediate-risk patients are favorable with the application of minimally

63 invasive ablative therapies, radiation therapy, or radical prostatectomy. However,

64 approximately 26% to 30% of prostate cancer patients will step into advanced and

65 metastatic stage within 5 years[2]. Although androgen deprivation therapy (ADT)

3

66   is available for these patients with advanced-stage [3], they still face a tricky

67   outcome, by rapidly progressing into the castration-resistant stage (CRPC), which

68   would cause the death of prostate cancer within 2 to 4 years[4]. For these CRPC

69   patients, who are accepted maximum androgen blockade therapy, their 5-year

70   overall survival (OS) rates are 25.4%, while the survival rates of patients merely

71   accepted androgen suppressed by surgery are only 1.8%[5]. Wallis *et al.* [6] also

72   reported the overall mortality (adjusted Hazard Ratio, HR) of high-risk prostate

73   cancer is higher than low-risk and intermediated risk patients (1.88 vs. 1.50, and

74   1.47). Currently, sipuleucel-T, abiraterone acetate, enzalutamide, cabazitaxel,

75   radium-223, and apalutamide are approved by the Food and Drug Administration

76   (FDA) and available for the CRPC patients [7-12].

77   Tumor microenvironment (TME) is the milieu of tumor and composites by a mass

78   of vessels, immune cells, stromal cells, mesenchymal cells, as well as the

79   cytokines and chemokines[13, 14], and it plays a crucial role during tumorigenesis

80   and progression. Many investigations have explored the role of TME in tumor

81   progression or prognostic prediction. In our previous study, we found that the M2

82   macrophage acts as a risk factor for prostate cancer patients[15]. Zhao *et al.*[16]

83   demonstrated the association between the high expression level of programmed

84   cell death 1 ligand 2 (PD-L2) and worse outcome of prostate cancer patients, as

85   well as the links with postoperative radiation therapy. Rodrigues *et al.*[17] also

86   illustrated the positive association between the defective mismatch repair

87   signatures and the over-activated of several immune checkpoints. Sipuleucel-T is

88   the first FDA approved immunotherapy option for prostate cancer patients, and the

89 recombinant fusion prostatic acid phosphatase (PAP) could active the antigen-

90 presenting cells (APCs) and remove the cells from the immunosuppressive milieu

91 of tumor [18, 19]. Otherwise, the anti-programmed cell death protein 1 (PD-1) and

92 anti-programmed cell death 1 ligand 1 (PD-L1) therapy is another potential

93 immunotherapy option for prostate cancer patients, which have been confirmed

94 offering benefits to patients with melanoma[20, 21], gastric cancer[22], non-small

95 cell lung cancer[23, 24], breast cancer[25], urothelial carcinoma[26]. However,

96 these immune checkpoint blockade (ICB) treatment only responds by part of the

97 patients, and the TME molecular features are tightly linked to the response of

98 chemoradiotherapy and ICB response [27, 28]. Therefore, it is essential to

99 investigate the sub-immunophenotypes in prostate cancer, which would guide the

100 potential immunotherapy for these patients.

101 In the current study, we employed the non-negative matrix factorization (NMF)

102 algorithm to discover the immune molecular patterns. Based on the immune

103 factors, three immunophenotypes were established with bulk tumor gene

104 expression profiles from public cohorts and a real-world AHMU-PC cohort. Our

105 results suggested that immune response drove outcomes in prostate cancer and

106 provided inspirations of immunotherapy for prostate cancer patients.

107 **Materials and Methods**

108 **Patient summary**

109 A total of 1,557 prostate cancer patients were enrolled in the current study, with

110 available gene expression profiles, clinicopathological features, and recurrent-free

111   survival records. The procedure of this study was demonstrated in **Figure 1**. The

112   Cancer Genome Atlas Prostate adenocarcinoma (TCGA-PRAD) cohort with 495

113   patients was set as the training cohort, while another three public cohorts,

114   Memorial Sloan-Kettering Cancer Center (MSKCC), GSE70770, GSE116918, and

115   GSE79021 cohorts were set as the validation cohorts, with a total of 993 prostate

116   cancer patients. What's more, we also collected the Formalin-fixed, paraffin-

117   embedded (FFPE) samples of 69 patients, with available recurrence-free survival

118   records from the Department of Urology, the First Affiliated Hospital of Anhui

119   Medical University (AHMU-PC cohort). The gene expression profiles were

120   determined by whole transcriptome sequencing based on Illumina NovaSeq

121   platforms with paired-end 150 bp sequencing strategy. The ethical approval for the

122   AHMU-PC cohort was obtained from the ethics committee of the First Affiliated

123   Hospital of Anhui Medical University (PJ2019-09-11). The detailed information of

124   all the enrolled cohorts was listed in **Supplementary Table 1**.

125   **Bioinformatic analyses**

126   In the training cohort, the gene expression profile was used to virtually microdissect

127   the patients to subgroups by the unsupervised non-negative matrix factorization

128   (NMF) algorithm as described in a prior study with Gene Pattern online tool [29,

129   30]. The NMF algorithm method could factorize the gene expression matrix V into

130   gene factor matrix W and sample factor matrix H (**Figure 1**) [31]. To select the

131   immune-related NMF factor, we employed the single-sample gene set enrichment

132   analysis (ssGSEA) to generate the immune score as described previously[32].

133   Then, the Immune and non-immune subtypes were dichotomized by the

134   GenePattern module 'NMFConsensus', with the gene expression of the top 150

135   exemplar genes of the immune-related NMF factor. The immune class was

136   furthermore divided into immune suppressed, and immune activated subtypes by

137   the nearest template prediction (GenePattern module 'NTP') of the activated

138   stroma [33]. Manually curated gene signatures representing various immune cell

139   types or host anti-tumor immunity were used to further characterize immune class

140   based on immunosuppressive or activated microenvironment *via* ssGSEA

141   (**Supplementary Table 2**). Copy number alterations (CNA), tumor-infiltrating

142   lymphocytes (TILs) were compared between different immune classes. To validate

143   the immunophenotypes obtained from the training cohort, the 150 differentially

144   expressed genes (DEGs) among immune and non-immune classes were used to

145   dichotomize the subgroups in external validation cohorts with GenePattern module

146   'NMFConsensus', and then revealed the immune activated and suppressed

147   subgroups by activated stroma signature. More details about the study protocol

148   were listed in the **Supplementary Materials and Methods**.

149   **Results**

150   **Discovering the immune-related factor and identifying the immune**

151   **subclasses of prostate cancer**

152   NMF algorithm was firstly employed to conduct the virtual microdissection of the

153   gene expression profile of the 495 prostate cancer patients derived from the

154   training TCGA-PRAD cohort. The second factor of the eleven expression patterns

155   (NMF clusters) was of immunologic relevance and obtained a relatively high

7

156   immune enrichment score (IES) than others (**Figure 2A**); therefore, we termed this

157   NMF factor as "immune factor". We chose the top 150 weighted genes as the

158   exemplar genes representing the second immune factor and performed the gene

159   ontology enrichment (**Supplementary Table 3**). The 150 exemplar genes were

160   most enriched in T cell activation, Leukocyte migration, and Lymphocyte

161   differentiation pathways (**Supplementary Figure 1**), and the top 5 exemplar genes

162   also showed positive relationships with B cell, CD8+ T cell, CD4+ T cell,

163   Macrophage, Neutrophil, and Dendritic cell (all, $P < 0.05$, **Supplementary Figure**

164   **2**).

165   The consensus clustering was performed to divide all the 495 patients, and the

166   multidimensional scaling (MDS) random forest was employed to define them into

167   immune and non-immune class **(Figure 2B-C).** Patients belonging to the immune

168   class showed significantly higher enrichment score of immune signals than the

169   non-immune class, including T cell, B cell, NK cell, and macrophage associated

170   signatures, as well as tertiary lymphoid structure (TLS), cytolytic activity score

171   (CYT) and IFN signatures (all, $P < 0.05$, **Figure 3, up panel**). Moreover, we

172   compared the difference of activated signaling by GSEA analysis between immune

173   class and non-immune class, and the results suggested that immune cell-

174   associated pathways, immune response pathways, proinflammatory pathways,

175   and tumor promotion pathways were enriched in the immune class [all false

176   discovery rate (FDR) < 0.05; **Figure 2D**]. Taken together the results from **Figure**

177   **2** and **Figure 3 up panel**, we identified the immune-related factor and exemplar

178   genes, which could define the immune subclasses in TCGA-PRAD.

8

179 **Two distinct immunophenotypes highlighted by different microenvironment**

180 **conditions**

181 Several studies reported that the heterogeneity of immune microenvironment was

182 existed in tumors, which showed the different infiltrating status of Treg cells,

183 myeloid-derived suppressor cell, or the different results of anti-PD-1

184 immunotherapy, and these tumors were defined as immune "hot" or "cold" groups,

185 respectively [34-36]. Therefore, we sought to explore the subphenotypes of

186 immune classes to distinguish the different immune response status. According to

187 the previously reported signature of activated stromal response, we revealed that

188 63.0% (126/200) of the immune class was characterized by a high stromal

189 enrichment score (SES) (**Figure 3, down panel**).

190 TGF-β is regarded as the central immune-suppressive mediator in the immune

191 microenvironment [37-39], and the high levels of extracellular matrix cytokines (C-

192 ECM), induced by the activated cancer-associated fibroblasts could also recruit

193 the immune suppressive cells [40-42]. Therefore, we evaluated the TGF-β-

194 associated signature and found that the WNT/TGF-β, TGF-β1 activation, and C-

195 ECM signatures were higher in the stromal activated subgroup than non-immune

196 class (all, $P < 0.05$, **Figure 3, down panel**). We termed the stromal activated

197 subgroup as the immune-suppressed subtype, while the remaining 27.0% of

198 patients (74/200) belonged to the immune activated subtype. Further, we also

199 observed an increased expression of IL11, TGFB1, and TGFB2 in immune-

200 suppressed subtype than immune activated subtype (all, $P < 0.05$,

201 **Supplementary Figure 3**), a result consistent with the previous publication [43].

202 A recent study suggested that PAK4 is enriched in non-responding tumor biopsies

203 [44], and in the current study, we found that PAK4 was higher expressed in the

204 immune-suppressed subtype than immune activated one (P = 0.037,

205 **Supplementary Figure 3**). Subsequently, we obtained the results that tumor-

206 infiltrating Tregs (TITR) signature (P < 0.01) and Treg cell signature (P = 0.017)

207 was mostly enriched in the immune-suppressed subtype (**Figure 3, down panel**).,

208 while the Th17 cell infiltration was higher in immune activated subtype (P = 0.034,

209 **Supplementary Figure 3**). Taken together the results from **Figure 3 and**

210 **Supplementary Figure 3**, we identified two distinct immunophenotypes, immune

211 suppressed, and immune activated, which were determined by different

212 microenvironment conditions.

213 **Correlations between immune class and copy number alteration, tumor‑**

214 **infiltrating lymphocytes enrichment, and lower cancer stemness**

215 The somatic mutations in tumor cells are the double-edged sword in the malignant

216 tumor. It could promote the tumorigenesis, while it could also be recognized by the

217 immune system and lead to forcefully acquired immunity. The immunogenicity of

218 anti-tumor immunes response is based on the non-self-antigen, which generated

219 by the somatic mutations of themselves [45]. The neoantigens could be captured

220 by the antigen presentation cells and then induced the activation of neoantigen‑

221 specific T cells, subsequently the tumor cells are killed by the tumor infiltration

222 lymphocyte (TIL) through the recognition of the neoantigen [46]. Here, we further

10

223   carried out immunophenotype analyses aiming to obtain deeper insights into the

224   immunological nature of the immune class.

225   In the TCGA cohort, the immune class showed a high burden of amplification in

226   both arm and focal levels ($P_{Arm-Amp}$ = 0.033, and $P_{Focal-Amp}$ = 0.015) rather than

227   deletion ($P_{Arm-del}$ = 0.54, $P_{Focal-del}$ = 0.14) (**Figure 4A-B**). Further, we found that the

228   CNA of several immune checkpoint genes, *PD-1*, *PD-L1*, *LGALS9*, and *CD48*,

229   were positively associated with the infiltration of immunocytes (**Supplementary**

230   **Figure 4**). As to the TMB and neoantigens, no differences were observed between

231   the immune and non-immune classes (P_{TMB} = 0.661, **Figure 4C**, P_{NeoAgs} = 0.271,

232   **Figure 4E**).

233   Notably, we revealed a different mutation landscape among the three

234   immunophenotypes based on the MutSigCV algorithm analysis (**Figure 4D,**

235   **Supplementary Table 3**). To be specific, the mutation frequencies of TP53 in the

236   immune class were higher than that of non-immune class (14.5% vs. 9.8%),

237   especially higher in the immune-suppressed subtype (19.0%, $P < 0.001$). As to

238   SPOP, fewer mutations were observed in suppressed subtype as compare with

239   both immune activated subtype and non-immune class (5.6% vs. 13.5%, and

240   13.2%, $P < 0.001$). In addition, we identified several immune class-specific

241   mutated genes, including *CHRNA6*, *KIAA1012*, *OR10R2*, *PLIN3*, *MOSPD3*,

242   *GMPR*, *DPPA5*, and *C10orf99* (all, $P < 0.05$).

243   Regarding TILs, we found a significantly higher density of TILs in immune class,

244   as compared with the non-immune class ($P = 0.001$, **Figure 4F**). The expression

11

245   of PD-L1 was also increased, along with the higher infiltration of CD8+ T cell, in

246   the immune class than non-immune class ($P < 0.001$, **Figure 4G**), consistent with

247   a previous study [47]. Moreover, Miranda *et al.*[48] reported a negative association

248   between stemness and immune response, and revealed that it is not readily

249   attributable to low neoantigen load. Here, we compared and revealed the lower

250   stemness, represented by mRNAsi [49], in immune class compared with the non-

251   immune class ($P < 0.001$, **Figure 4H**). Taken together the results from **Figure 4**,

252   **Supplementary Figure 4**, and **Supplementary Table 3**, our results reveal that

253   the immune class is correlated with significantly higher copy number alterations,

254   higher TILs enrichment, but not with TMB and neoantigens.

255   **Validation of the three immunophenotypes in external cohorts**

256   To confirm the accuracy of the NMF algorithm and activated stromal signature-

257   based immunophenotypes, we included an additional 993 prostate cancer patients

258   with available gene expression profiles and clinicopathological features

259   (**Supplementary Table 1**). 150 upregulated genes were identified between

260   Immune and non-Immune Classes (**Supplementary Table 5**), the top 5 DEGs

261   showed positive relationships with B cell, CD8+ T cell, CD4+ T cell, Macrophage,

262   Neutrophil, and Dendritic cell (all, $P < 0.05$, **Supplementary Figure 5**). Then, the

263   immune classifier was applied to identify the immune classes in three external

264   datasets using the GenePattern module "NMFConsensus" referring to the 150

265   genes. The immune class was furthermore divided into immune suppressed and

266   immune activated subtypes by the nearest template prediction of activated stroma

267   signature.

12

268   In GSE70770 cohort, 51.7% (105/203) patients were identified as the non-

269   immune class, 42 patients (20.7%) in immune activated subtype and 56 patients

270   (27.6%) in the immune-suppressed subtype (**Figure 5**, **left panel**). As to the 248

271   patients from the GSE116918 cohort, 54.5% (140/248) patients belonged to the

272   non-immune class, 75 patients (30.2%) divided into an immune-suppressed

273   subtype, while the other 33 patients (13.3%) belonged to immune activated

274   subtype (**Figure 5**, **middle panel**). In the MSKCC cohort, 73 patients (52.1%) were

275   identified as the non-immune class, while 34 (24.3%) and 33 (23.6%) patients

276   belonged to activation and suppressed subtypes, respectively (**Figure 5**, **right**

277   **panel**). Another 402 patients extracted from the GSE79021 cohort also displayed

278   similar results, 21.6% (87/402) patients belonged to immune activated subtype,

279   18.7% (75/402) in the immune-suppressed subtype, and the remaining 240

280   patients were with non-immune status **(Supplementary Figure 6).** For the results

281   of immune signatures in these four external validation cohorts, the IES and

282   immune signaling signature were significantly enriched in the immune class (all, P

283   < 0.05), as well as the ssGSEA results of T cell, B cell, Macrophage, TLS, CYT

284   and IFN signatures (all, $P < 0.05$). Meanwhile, the subtypes of activation and

285   suppressed were divided by the stromal activation signature generated by the NTP

286   method, and the immune-suppressed subtype showed a higher SES than the

287   immune activated subtype in these three external cohorts (all, $P < 0.05$). Further,

288   the higher enrichments of Treg cells, TITR, MDSC, WNT/TGFβ, and C-ECM

289   signatures were identified in the immune-suppressed subtype than immune

290   activated subtype in these three external cohorts (all, $P < 0.05$). Taken together,

13

291 combined results from **Figure 5 and Supplementary Figure 6**, our results suggest

292 that the 150 DEGs are stable markers that could be used to distinguish immune or

293 non-immune subclass in prostate cancer.

294 **Immune activated linked to a favorable recurrence-free survival and anti-PD-**

295 **1 immunotherapy**

296 The clinicopathological features are important standards to demonstrate the

297 malignant degree of prostate cancer. Here, we explored the distributions of the

298 three immunophenotypes in different clinicopathological features. Patients in the

299 immune-suppressed class were more at advanced stage than other two

300 subclasses in the TCGA-PRAD cohort [Gleason score > 7 (48/126, 61.9%, $P <$

301 0.001), T stage > T2 (99/125, 79.2%, $P < 0.001$)] (**Supplementary Figure 7**).

302 Similar results were obtained in the GSE116918 and GSE70770 cohorts

303 (**Supplementary Figure 7**).

304 We also sought to integrate the immunophenotypes with the prior established

305 immune molecular features. Thorsson *et al.*[50] generated a six-subtype immune

306 molecular feature, including wound healing, IFN-γ dominant, inflammatory,

307 lymphocyte depleted, immunologically quiet, and TGF-β dominant. We revealed

308 that most prostate cancer patients belong to the inflammatory group, and the

309 immune activated subtype ranked the highest proportion in the inflammatory group

310 (46/50, 92.0%), followed by the immune-suppressed subtype (85/114, 74.6%), and

311 non-immune class (176/241, 73.0%) ($P < 0.001$, **Supplementary Figure 8**). Zhao

312 et al.[51] defined the molecular subtypes of pan-cancer with the PAM50 classifier,

14

313   which approved by the FDA for the clinical prognostic evaluation of breast

314   cancer[52]. We classified the 495 patients in the TCGA-PRAD cohort into Luminal

315   A, Luminal B, and Basal-like group. We revealed that the immune activation

316   subtype contained more Luminal A-like patients, while the immune suppression

317   subtype contained more Luminal B-like patients (P < 0.001, **Supplementary**

318   **Figure 9**).

319   The different RFS according to immune molecular subgroups were also

320   assessed. In the TCGA-PRAD cohort, with patients younger than 60 years old, we

321   observed that the immune activated subtype showed a favorable RFS, an immune-

322   suppressed subtype with the worse RFS, and non-immune class along with the

323   medial recurrence outcome (P=0.15, **Figure 6A**). The similar results could also be

324   concluded in GSE70770 (P=0.0065, **Figure 6B**), GSE116918 (P=0.034, **Figure**

325   **6C**) and MSKCC (P=0.030, **Figure 6D**) cohort that the immune activated subtype

326   showed the best RFS outcome in all the three immunophenotypes, while the

327   patients in immune-suppressed subtype showed the shortest average RFS time.

328   Finally, we tested the potential capacity of the immune molecular classification

329   system in selecting candidate patients to receive anti-PD-(L)1 immunotherapy.

330   SubMap analysis, which is used to identify common subtypes in independent

331   datasets, manifested that prostate cancer samples in immune activated subtype

332   shared a similar immune-related gene expression profile to that of melanoma

333   patients responsive to anti-PD-1 immunotherapy (Bonferroni-corrected P = 0.0079,

334   **Supplementary Figure 10**). Taken together of the results from **Figure 6** and

335   **Supplementary Figure 7-10,** we detailly explored the clinicopathological and

15

336   molecular distinctions among the three immunophenotypes, patients with the

337   immune activated statues showed the best outcome and could benefit more from

338   the anti-PD-1/PD-L1 immunotherapy.

339   **Reappearing the three immunophenotypes upon a real-world AHMU-PC**

340   **cohort**

341   In the AHMU-PC cohort, we retrospectively collected the FFPE tissue of 69

342   patients with available clinicopathological features and received a long-time follow-

343   up and performed whole transcriptome sequencing to obtain the gene expression

344   profile. With the help of "NMFConsensus", 47.8% (33/69) patients were revealed

345   with high IES and assigned into the immune class, while the other 52.2% patients

346   belonged to non-immune class. Further, the immune class was subsequently

347   classified into immune activated (14/69, 20.3%) and suppressed (19/69, 27.5%)

348   subtypes. Similar to the results obtained above, the patients in the immune class

349   showed a higher enrichment score of T cell, B cell, macrophages, TLS, CYT, and

350   IFN signatures (all, $P < 0.05$) than the non-immune class. And the immune-

351   suppressed subtype displayed a high score of SESs, TITR, MDSC, and C-ECM

352   signature (all, $P < 0.05$, **Figure 7A**). We also employed the Kaplan-Meier analysis

353   to determine the RFS outcome differences among the three immunophenotypes.

354   Consistently, the immune-suppressed subtype showed the worst recurrence-free

355   survival outcome than the immune activated and non-immune subgroups ($P =$

356   0.0083, **Figure 7B**). Further, patients in the immune activated subtype were mostly

357   enriched at the early pathological stage, assessed by Gleason score (92.3% vs.

358   44.4%, 48.57%, $P = 0.0127$, **Supplementary Figure 11**) and pathology T stage

16

359   (92.9% vs. 65.0%, 75.0%, *P* = 0.368, **Supplementary Figure 11**). Patients in the

360   immune activated subgroup of the AHMU-PC cohort seemed to benefit more from

361   the anti-PD-1/PD-L1 immunotherapy than the non-immune activated class

362   (Bonferroni-corrected *P* = 0.0399, **Figure 7C)**. Taken together of **Figure 7** and

363   **Supplementary Figure 11**, we reappeared the three immunophenotypes in the

364   AHMU-PC cohort, patients in the immune-suppressed showed the worst

365   recurrence-free survival outcome, and patients in the immune activated subtype

366   could benefit more from anti-PD-1/PD-L1 therapy.

367   **Discussion**

368   CRPC patients always face the most terrible symptoms and complications than

369   early-stage patients, including short survival, bone metastases induced bone pain,

370   spinal cord compression, ureteric obstruction, and renal failure [53-55]. Several

371   therapeutic agents are approved for the treatment of CRPC, including the immune-

372   associated sipuleucel-T, while the potential treatment of anti-PD-1/PD-L1 is still

373   under the clinical evaluation [56]. Immune checkpoints promote or inhibit factors in

374   TME, and several immune checkpoints could help the tumor escape from the

375   recognition and attack of the host immune system[57, 58]. The anti-PD-1/PD-L1

376   therapy is applied in several malignancy tumors, but could only benefit part of

377   patients. In the IMvigor210 trial, only 68/248 (27.4%) of bladder cancer patients

378   benefited from the treatment of PD-L1 inhibitor (atezolizumab). For gastric tumors,

379   only 11.6% of enrolled patients responded to the pembrolizumab monotherapy in

380   the KEYNOTE-059 trial and objective response rate of nivolumab in ATT RAC

381   TION-2 trial was only 11.2% [22, 59]. Therefore, it is essential to provide a

17

382   comprehensive decipherment of the prostate cancer immune microenvironment,

383   which could help find suitable patients to receive immunotherapy.

384   NMF approach is a virtual separation approach that has been applied

385   successfully in several fields including image and pattern recognition, signal

386   processing and text mining[60], as well as been applied to obtain novel insights

387   into cancer type discovery based on gene expression profiles by identifying the

388   exemplar genes [33, 61]. In the current study, we proposed a robust

389   immunogenomic classification system of prostate cancer based on the NMF

390   algorithm. The immune exemplar genes and stromal activation signature

391   supported us to defined three immunophenotypes: immune activation, immune

392   suppression, and non-immune classes. A similar method to revealed the

393   immunophenotypes was applied and validated in hepatocellular carcinoma, gastric

394   cancer, and head and neck squamous cell carcinoma[62-64]. Initially, we observed

395   the landscape of immune class distributions in prostate cancer derived from the

396   TCGA-PRAD cohort. Of the 495 patients, 40.4% of them belonged to the immune

397   class, along with a higher enrichment of immunocytes, cytolytic activity, and IFN

398   signaling than non-immune class, and these signatures are also highly resembled

399   in response to immunotherapy[65, 66]. Subsequently, we dissected the immune

400   class into immune activated and immune-suppressed subtypes based on the

401   stromal activated signature. 14.9% of the overall patients belonged to the immune

402   activated subtype along with the lower enrichment of SES, WNT/TGF-β, C-ECM,

403   and TITR signatures, while the remaining 25.5% were immune suppression. The

404   similar immunophenotypes were also validated in four external cohorts. The

18

405   immune activated subtype was 20.7% in the GSE70770 cohort, 13.3% in the

406   GSE116918 cohort, 24.3% in the MSKCC cohort, 21.6% in the GSE79021 cohort,

407   and 20.3% in the AHMU-PC cohort. All these results indicate that only about 13.3-

408   24.3% of overall patients could benefit from immunotherapy.

409   PAM50 classifier was first described by Perou *et al.*[67], who subclassified

410   breast cancer into four subtypes, including Luminal A, Luminal B, HER2-enriched,

411   and Basal-like. The FDA approved the application of the PAM50 classifier in

412   clinical prognostic evaluation of breast cancer patients in 2013 [52, 67, 68]. PAM50

413   subtypes also display different prognostic outcomes and responses to clinical

414   therapy in breast and bladder cancer [69, 70]. Supplement to Zhao *et al.*'s work

415   about the PAM50 classifier applying to prostate cancer patients, we classified the

416   495 patients in the TCGA-PRAD training cohort into Luminal A, Luminal B, and

417   Basal-like   subgroups.   After   comparing   the   distributions   of   three

418   immunophenotypes and PAM50 subtypes, we revealed that the immune activated

419   class contained more Luminal A like patients, while the immune-suppressed

420   subtype contained more Luminal B like patients. Besides, our results were

421   consistent with Zhu *et al.*'s work[71] that the Luminal A patients showed a higher

422   expression of immune checkpoint genes (PD-L1 and CTLA-4) and chemokine

423   genes (CXCL9 and CXCL10). Poudel *et al.*[72] also reported the heterogeneity of

424   Luminal A-like breast cancer patients. The inflammatory Luminal A subtype is

425   enriched with highly immune-associated signatures, as well as the increased

426   expression of immune checkpoints (PD-L1, CTLA-4, LAG3, and PDCD1). Recently,

427   Thorsson *et al.*[50] also generated the pan-cancer atlas of TCGA, which identified

19

428   six pan-cancer immunes. For prostate cancer patients, most of them belonged to

429   the inflammatory subtype, and the distributions were similar in immune class and

430   non-immune class. Interestingly, after dividing the immune class into activated and

431   suppressed subtypes, the inflammatory subtype accounted for the major part of

432   immune activated patients (92.0%). The inflammatory subtype was defined by the

433   elevated Th17 cells [50], and we also revealed an increased infiltration of Th17

434   cells in the immune-activated subtype. Derhovanessian *et al.*[73] reported that

435   Th17 cells were higher in those patients who are responsive to immunotherapy

436   than in non-responders, and negatively correlated with tumor stages.

437   The CNAs were decreased as compared with non-immune class in both arm

438   and focal level as reported in the immunophenotype study in gastric cancer and

439   head and neck carcinoma[62, 63]. However, we observed a different phenomenon

440   that the arm-level of CNA in immune activated subtype was increased, which might

441   be linked to the elevated infiltration of immunocytes, increased release of cytokines,

442   and the CNA of immune checkpoint genes in prostate cancer [74]. No differences

443   concerning TMB and neoantigens between the immune class and the non-immune

444   class were found in our study. Although the somatic mutation frequencies of

445   prostate cancer are dramatically lower than those in melanoma and non-small-cell

446   lung cancer[75, 76], Subudhi *et al.*[77] reported that part of the metastatic

447   castration-resistant prostate cancer patients who received ipilimumab treatment

448   can still benefit from the immunotherapy with the median number of

449   nonsynonymous somatic mutations of 76.

450 Meanwhile, we presented the gene somatic mutation landscape in the three

451 immunophenotypes. The mutations of TP53 were mostly observed in non-immune

452 class, and the proportion was only 5.4% in the immune activated subtype. Jiang *et*

453 *al.*[78] demonstrated that the TP53 mutation results in the depressed immune

454 activity in gastric cancer, and the less active immune pathways and cell types are

455 observed in TP53-mutated gastric cancer patients. Carlisle *et al.* [79] also reported

456 TP53 mutation correlates with the poor efficacy of immunotherapy after adjusting

457 PD-L1 expression in NSCLC. The mutations of SPOP in the immune activated

458 subtype is more than the immune-suppressed subtype in our study. Zhang *et al.*[80]

459 demonstrated that SPOP promotes the ubiquitin-mediated degradation of PD-L1,

460 and the mutant SPOP leads to elevated PD-L1 levels in prostate cancer patients.

461 The novel defined three immunophenotypes that are essential for selecting

462 suitable immunotherapies for prostate cancer patients. Patients in the immune

463 activated subtype could benefit more from the single ICB treatment, while the

464 immune-suppressed patients could benefit from the TGF-β inhibitors plus ICB

465 therapy. Regarding the issue, the fusion protein M7824, comprising TGF-β Trap

466 linked to the C-terminus of the human anti-PD-L1 heavy chain, is more suitable for

467 immune-suppressed patients by decreasing TGFβ-induced signaling and

468 promoting the activations of CD8+ T cells and NK cells [81]. For the non-immune

469 class, the combination of anti-CTLA-4 and anti-PD-1/PD-L1 therapy, which attracts

470 the infiltration of immune cells in TME and keep the turn-on status of them, might

471 reverse the non-responders[82-84].

472 **Conclusion**

21

473 We established and validated a novel classifier of immunophenotypes based on

474 the expression profiles of 1,557 prostate cancer patients, including 69 real-world

475 prostate cancer patients from our center. The NMF algorithm microdissects

476 patients to immune activated, immune suppressed, and non-immune classes.

477 Patients in the immune-activated subtype might benefit more from anti-PD-1/PD-

478 L1 therapy, and in the immune-suppressed group are more suitable for anti-TGF-

479 β plus anti-PD-1/PD-L1 therapy. To conclude, our findings suggest that immune

480 response drives outcomes in prostate cancer, and offers inspiration for

481 immunotherapy in prostate cancer patients.

482 **Abbreviations**

483 Androgen deprivation therapy, ADT; castration-resistant stage, CRPC; overall survival,

484 OS; the Food and Drug Administration, FDA; tumor microenvironment, TME; programmed

485 cell death 1 ligand 2, PD-L2; prostatic acid phosphatase, PAP; antigen-presenting cells,

486 APCs; programmed cell death protein 1, PD-1; programmed cell death 1 ligand 1, PD-L1;

487 immune checkpoint blockade, ICB; non-negative matrix factorization, NMF; The Cancer

488 Genome Atlas-prostate adenocarcinoma, TCGA-PRAD; Memorial Sloan-Kettering

489 Cancer Center, MSKCC; formalin-fixed paraffin-embedded, FFPE; Anhui medical

490 university-prostate cancer cohort, AHMU-PC cohort; single-sample gene set enrichment

491 analysis, ssGSEA; copy number alterations, CNA; tumor-infiltrating lymphocytes, TILs;

492 differentially expressed genes, DEGs; immune enrichment score, IES; multidimensional

493 scaling, MDS; tertiary lymphoid structure, TLS; cytolytic activity score, CYT; false

494 discovery rate, FDR; stromal enrichment score, SES; extracellular matrix cytokines, C-

495 ECM; tumor-infiltrating Tregs, TITR.

Conflicts of interest statement

None.

Acknowledgments

Funding support

Author contribution

Conception and Design: Jialin Meng, Meng Zhang, and Chaozhao Liang. Collection and Assembly of Data: Yujie Zhou, Xiaofan Lu, Zichen Bian, Song Fan, Jun Zhou. Data Analysis and Interpretation: Yujie Zhou, Xiaofan Lu, Yiding Chen, Li Zhang, Zongyao Hao. Manuscript Writing: Jialin Meng, Meng Zhang, Yujie Zhou, Yiding Chen. Final Approval of Manuscript: All the authors.

Ethics

The research contents and research programs were reviewed and approved by the Ethics Committee of the First Affiliated Hospital of Anhui Medical University (PJ-2019-09-11).

23

References:

1. Ferlay J, Colombet M, Soerjomataram I, Mathers C, Parkin DM, Pineros M, Znaor A, Bray F: **Estimating the global cancer incidence and mortality in 2018: GLOBOCAN sources and methods.** *Int J Cancer* 2019, **144:**1941-1953.

2. Steele CB, Li J, Huang B, Weir HK: **Prostate cancer survival in the United States by race and stage (2001-2009): Findings from the CONCORD-2 study.** *Cancer* 2017, **123 Suppl 24:**5160-5177.

3. Harris WP, Mostaghel EA, Nelson PS, Montgomery B: **Androgen deprivation therapy: progress in understanding mechanisms of resistance and optimizing androgen depletion.** *Nat Clin Pract Urol* 2009, **6:**76-85.

4. Omlin A, Pezaro C, Mukherji D, Mulick Cassidy A, Sandhu S, Bianchini D, Olmos D, Ferraldeschi R, Maier G, Thompson E, et al: **Improved survival in a cohort of trial participants with metastatic castration-resistant prostate cancer demonstrates the need for updated prognostic nomograms.** *Eur Urol* 2013, **64:**300-306.

5. **Maximum androgen blockade in advanced prostate cancer: an overview of the randomised trials. Prostate Cancer Trialists' Collaborative Group.** *Lancet* 2000, **355:**1491-1498.

6. Wallis CJD, Saskin R, Choo R, Herschorn S, Kodama RT, Satkunasivam R, Shah PS, Danjoux C, Nam RK: **Surgery Versus Radiotherapy for Clinically-localized Prostate Cancer: A Systematic Review and Meta-analysis.** *Eur Urol* 2016, **70:**21-30.

7. Kantoff PW, Higano CS, Shore ND, Berger ER, Small EJ, Penson DF, Redfern CH, Ferrari AC, Dreicer R, Sims RB, et al: **Sipuleucel-T immunotherapy for castration-resistant prostate cancer.** *N Engl J Med* 2010, **363:**411-422.

8. Ryan CJ, Smith MR, Fizazi K, Saad F, Mulders PF, Sternberg CN, Miller K, Logothetis CJ, Shore ND, Small EJ, et al: **Abiraterone acetate plus prednisone versus placebo plus prednisone in chemotherapy-naive men with metastatic castration-resistant prostate cancer (COU-AA-302): final overall survival analysis of a randomised, double-blind, placebo-controlled phase 3 study.** *Lancet Oncol* 2015, **16:**152-160.

9. Beer TM, Armstrong AJ, Rathkopf DE, Loriot Y, Sternberg CN, Higano CS, Iversen P, Bhattacharya S, Carles J, Chowdhury S, et al: **Enzalutamide in metastatic prostate cancer before chemotherapy.** *N Engl J Med* 2014, **371:**424-433.

10. de Bono JS, Oudard S, Ozguroglu M, Hansen S, Machiels JP, Kocak I, Gravis G, Bodrogi I, Mackenzie MJ, Shen L, et al: **Prednisone plus cabazitaxel or mitoxantrone for metastatic castration-resistant prostate cancer progressing after docetaxel treatment: a randomised open-label trial.** *Lancet* 2010, **376:**1147-1154.

11. Parker C, Nilsson S, Heinrich D, Helle SI, O'Sullivan JM, Fossa SD, Chodacki A, Wiechno P, Logue J, Seke M, et al: **Alpha emitter radium-223 and survival in metastatic prostate cancer.** *N Engl J Med* 2013, **369:**213-223.

12. Smith MR, Saad F, Chowdhury S, Oudard S, Hadaschik BA, Graff JN, Olmos D, Mainwaring PN, Lee JY, Uemura H, et al: **Apalutamide Treatment and Metastasis-free Survival in Prostate Cancer.** *N Engl J Med* 2018, **378:**1408-1418.

13. Hanahan D, Coussens LM: **Accessories to the crime: functions of cells recruited to the tumor microenvironment.** *Cancer Cell* 2012, **21:**309-322.

14. Casey SC, Amedei A, Aquilano K, Azmi AS, Benencia F, Bhakta D, Bilsland AE, Boosani CS, Chen S, Ciriolo MR, et al: **Cancer prevention and therapy through**

566 the modulation of the tumor microenvironment. *Semin Cancer Biol* 2015, **35**
567 **Suppl:**S199-S223.
568 15. Meng J, Liu Y, Guan S, Fan S, Zhou J, Zhang M, Liang C: **The establishment of**
569 **immune infiltration based novel recurrence predicting nomogram in prostate**
570 **cancer.** *Cancer Med* 2019, **8:**5202-5213.
571 16. Zhao SG, Lehrer J, Chang SL, Das R, Erho N, Liu Y, Sjostrom M, Den RB,
572 Freedland SJ, Klein EA, et al: **The Immune Landscape of Prostate Cancer and**
573 **Nomination of PD-L2 as a Potential Therapeutic Target.** *J Natl Cancer Inst*
574 2019, **111:**301-310.
575 17. Nava Rodrigues D, Rescigno P, Liu D, Yuan W, Carreira S, Lambros MB, Seed G,
576 Mateo J, Riisnaes R, Mullane S, et al: **Immunogenomic analyses associate**
577 **immunological alterations with mismatch repair defects in prostate cancer.**
578 *J Clin Invest* 2018, **128:**4441-4453.
579 18. Small EJ, Schellhammer PF, Higano CS, Redfern CH, Nemunaitis JJ, Valone FH,
580 Verjee SS, Jones LA, Hershberg RM: **Placebo-controlled phase III trial of**
581 **immunologic therapy with sipuleucel-T (APC8015) in patients with**
582 **metastatic, asymptomatic hormone refractory prostate cancer.** *J Clin Oncol*
583 2006, **24:**3089-3094.
584 19. Small EJ, Fratesi P, Reese DM, Strang G, Laus R, Peshwa MV, Valone FH:
585 **Immunotherapy of hormone-refractory prostate cancer with antigen-loaded**
586 **dendritic cells.** *J Clin Oncol* 2000, **18:**3894-3903.
587 20. Pollack MH, Betof A, Dearden H, Rapazzo K, Valentine I, Brohl AS, Ancell KK,
588 Long GV, Menzies AM, Eroglu Z, et al: **Safety of resuming anti-PD-1 in patients**
589 **with immune-related adverse events (irAEs) during combined anti-CTLA-4**
590 **and anti-PD1 in metastatic melanoma.** *Ann Oncol* 2018, **29:**250-255.
591 21. Larkin J, Chiarion-Sileni V, Gonzalez R, Grob JJ, Cowey CL, Lao CD, Schadendorf
592 D, Dummer R, Smylie M, Rutkowski P, et al: **Combined Nivolumab and**
593 **Ipilimumab or Monotherapy in Untreated Melanoma.** *N Engl J Med* 2015,
594 **373:**23-34.
595 22. Fuchs CS, Doi T, Jang RW, Muro K, Satoh T, Machado M, Sun W, Jalal SI, Shah
596 MA, Metges JP, et al: **Safety and Efficacy of Pembrolizumab Monotherapy in**
597 **Patients With Previously Treated Advanced Gastric and Gastroesophageal**
598 **Junction Cancer: Phase 2 Clinical KEYNOTE-059 Trial.** *JAMA Oncol* 2018,
599 **4:**e180013.
600 23. Fehrenbacher L, Spira A, Ballinger M, Kowanetz M, Vansteenkiste J, Mazieres J,
601 Park K, Smith D, Artal-Cortes A, Lewanski C, et al: **Atezolizumab versus**
602 **docetaxel for patients with previously treated non-small-cell lung cancer**
603 **(POPLAR): a multicentre, open-label, phase 2 randomised controlled trial.**
604 *Lancet* 2016, **387:**1837-1846.
605 24. Barlesi F, Vansteenkiste J, Spigel D, Ishii H, Garassino M, de Marinis F, Ozguroglu
606 M, Szczesna A, Polychronis A, Uslu R, et al: **Avelumab versus docetaxel in**
607 **patients with platinum-treated advanced non-small-cell lung cancer**
608 **(JAVELIN Lung 200): an open-label, randomised, phase 3 study.** *Lancet Oncol*
609 2018, **19:**1468-1479.
610 25. Schmid P, Adams S, Rugo HS, Schneeweiss A, Barrios CH, Iwata H, Dieras V,
611 Hegg R, Im SA, Shaw Wright G, et al: **Atezolizumab and Nab-Paclitaxel in**
612 **Advanced Triple-Negative Breast Cancer.** *N Engl J Med* 2018, **379:**2108-2121.
613 26. Powles T, Duran I, van der Heijden MS, Loriot Y, Vogelzang NJ, De Giorgi U,
614 Oudard S, Retz MM, Castellano D, Bamias A, et al: **Atezolizumab versus**
615 **chemotherapy in patients with platinum-treated locally advanced or**

616   metastatic urothelial carcinoma (IMvigor211): a multicentre, open-label,
617   phase 3 randomised controlled trial. *Lancet* 2018, **391:**748-757.
618 27. Wang Z, Tang Y, Tan Y, Wei Q, Yu W: **Cancer-associated fibroblasts in
619   radiotherapy: challenges and new opportunities.** *Cell Commun Signal* 2019,
620   **17:**47.
621 28. Havel JJ, Chowell D, Chan TA: **The evolving landscape of biomarkers for
622   checkpoint inhibitor immunotherapy.** *Nat Rev Cancer* 2019, **19:**133-150.
623 29. Brunet JP, Tamayo P, Golub TR, Mesirov JP: **Metagenes and molecular pattern
624   discovery using matrix factorization.** *Proc Natl Acad Sci U S A* 2004, **101:**4164-
625   4169.
626 30. Reich M, Liefeld T, Gould J, Lerner J, Tamayo P, Mesirov JP: **GenePattern 2.0.**
627   *Nat Genet* 2006, **38:**500-501.
628 31. Lee DD, Seung HS: **Learning the parts of objects by non-negative matrix
629   factorization.** *Nature* 1999, **401:**788-791.
630 32. Yoshihara K, Shahmoradgoli M, Martinez E, Vegesna R, Kim H, Torres-Garcia W,
631   Trevino V, Shen H, Laird PW, Levine DA, et al: **Inferring tumour purity and
632   stromal and immune cell admixture from expression data.** *Nat Commun* 2013,
633   **4:**2612.
634 33. Moffitt RA, Marayati R, Flate EL, Volmar KE, Loeza SG, Hoadley KA, Rashid NU,
635   Williams LA, Eaton SC, Chung AH, et al: **Virtual microdissection identifies
636   distinct tumor- and stroma-specific subtypes of pancreatic ductal
637   adenocarcinoma.** *Nat Genet* 2015, **47:**1168-1178.
638 34. Rotte A, Jin JY, Lemaire V: **Mechanistic overview of immune checkpoints to
639   support the rational design of their combinations in cancer immunotherapy.**
640   *Ann Oncol* 2018, **29:**71-83.
641 35. Galon J, Bruni D: **Approaches to treat immune hot, altered and cold tumours
642   with combination immunotherapies.** *Nat Rev Drug Discov* 2019, **18:**197-218.
643 36. Tanaka A, Sakaguchi S: **Regulatory T cells in cancer immunotherapy.** *Cell Res*
644   2017, **27:**109-118.
645 37. Batlle E, Massague J: **Transforming Growth Factor-beta Signaling in Immunity
646   and Cancer.** *Immunity* 2019, **50:**924-940.
647 38. Yang L, Pang Y, Moses HL: **TGF-beta and immune cells: an important
648   regulatory axis in the tumor microenvironment and progression.** *Trends
649   Immunol* 2010, **31:**220-227.
650 39. Wahl SM, Wen J, Moutsopoulos N: **TGF-beta: a mobile purveyor of immune
651   privilege.** *Immunol Rev* 2006, **213:**213-227.
652 40. Liu T, Han C, Wang S, Fang P, Ma Z, Xu L, Yin R: **Cancer-associated fibroblasts:
653   an emerging target of anti-cancer immunotherapy.** *J Hematol Oncol* 2019,
654   **12:**86.
655 41. Chakravarthy A, Khan L, Bensler NP, Bose P, De Carvalho DD: **TGF-beta-
656   associated extracellular matrix genes link cancer-associated fibroblasts to
657   immune evasion and immunotherapy failure.** *Nat Commun* 2018, **9:**4692.
658 42. Monteran L, Erez N: **The Dark Side of Fibroblasts: Cancer-Associated
659   Fibroblasts as Mediators of Immunosuppression in the Tumor
660   Microenvironment.** *Front Immunol* 2019, **10:**1835.
661 43. Xu DH, Zhu Z, Wakefield MR, Xiao H, Bai Q, Fang Y: **The role of IL-11 in
662   immunity and cancer.** *Cancer Lett* 2016, **373:**156-163.
663 44. Gajewski TF, Fessler J: **PAK4 as a cancer immune-evasion target.** *Nature
664   Cancer* 2020, **1:**18-19.
665 45. Schumacher TN, Schreiber RD: **Neoantigens in cancer immunotherapy.**
666   *Science* 2015, **348:**69-74.

667 46. Chen DS, Mellman I: **Oncology meets immunology: the cancer-immunity**
668   **cycle.** *Immunity* 2013, **39:**1-10.
669 47. Thompson ED, Zahurak M, Murphy A, Cornish T, Cuka N, Abdelfatah E, Yang S,
670   Duncan M, Ahuja N, Taube JM, et al: **Patterns of PD-L1 expression and CD8 T**
671   **cell infiltration in gastric adenocarcinomas and associated immune stroma.**
672   *Gut* 2017, **66:**794-801.
673 48. Miranda A, Hamilton PT, Zhang AW, Pattnaik S, Becht E, Mezheyeuski A, Bruun
674   J, Micke P, de Reynies A, Nelson BH: **Cancer stemness, intratumoral**
675   **heterogeneity, and immune response across cancers.** *Proc Natl Acad Sci U S*
676   *A* 2019, **116:**9020-9029.
677 49. Malta TM, Sokolov A, Gentles AJ, Burzykowski T, Poisson L, Weinstein JN,
678   Kaminska B, Huelsken J, Omberg L, Gevaert O, et al: **Machine Learning**
679   **Identifies Stemness Features Associated with Oncogenic Dedifferentiation.**
680   *Cell* 2018, **173:**338-354 e315.
681 50. Thorsson V, Gibbs DL, Brown SD, Wolf D, Bortone DS, Ou Yang TH, Porta-Pardo
682   E, Gao GF, Plaisier CL, Eddy JA, et al: **The Immune Landscape of Cancer.**
683   *Immunity* 2018, **48:**812-830 e814.
684 51. Zhao SG, Chen WS, Das R, Chang SL, Tomlins SA, Chou J, Quigley DA, Dang
685   HX, Barnard TJ, Mahal BA, et al: **Clinical and Genomic Implications of Luminal**
686   **and Basal Subtypes Across Carcinomas.** *Clin Cancer Res* 2019, **25:**2450-2457.
687 52. Nielsen T, Wallden B, Schaper C, Ferree S, Liu S, Gao D, Barry G, Dowidar N,
688   Maysuria M, Storhoff J: **Analytical validation of the PAM50-based Prosigna**
689   **Breast Cancer Prognostic Gene Signature Assay and nCounter Analysis**
690   **System using formalin-fixed paraffin-embedded breast tumor specimens.**
691   *BMC Cancer* 2014, **14:**177.
692 53. Gater A, Abetz-Webb L, Battersby C, Parasuraman B, McIntosh S, Nathan F,
693   Piault EC: **Pain in castration-resistant prostate cancer with bone metastases:**
694   **a qualitative study.** *Health Qual Life Outcomes* 2011, **9:**88.
695 54. Divya Yerramilli EW, Emma Turner, Grace Young, Ryan David Nipp, Jenny
696   Donovan, Freddie Hamdy, Neal David, Richard Martin, Jennifer S. Temel, Anthony
697   L. Zietman: **Cancer-related morbidity at the end of life in men with prostate**
698   **cancer.** *Journal of Clinical Oncology* 2018, **36:**5042-5042.
699 55. Kirby M, Hirst C, Crawford ED: **Characterising the castration-resistant prostate**
700   **cancer population: a systematic review.** *Int J Clin Pract* 2011, **65:**1180-1192.
701 56. Nuhn P, De Bono JS, Fizazi K, Freedland SJ, Grilli M, Kantoff PW, Sonpavde G,
702   Sternberg CN, Yegnasubramanian S, Antonarakis ES: **Update on Systemic**
703   **Prostate Cancer Therapies: Management of Metastatic Castration-resistant**
704   **Prostate Cancer in the Era of Precision Oncology.** *Eur Urol* 2019, **75:**88-99.
705 57. Carosella ED, Ploussard G, LeMaoult J, Desgrandchamps F: **A Systematic**
706   **Review of Immunotherapy in Urologic Cancer: Evolving Roles for Targeting**
707   **of CTLA-4, PD-1/PD-L1, and HLA-G.** *Eur Urol* 2015, **68:**267-279.
708 58. Topalian SL, Weiner GJ, Pardoll DM: **Cancer immunotherapy comes of age.** *J*
709   *Clin Oncol* 2011, **29:**4828-4836.
710 59. Kang YK, Boku N, Satoh T, Ryu MH, Chao Y, Kato K, Chung HC, Chen JS, Muro
711   K, Kang WK, et al: **Nivolumab in patients with advanced gastric or gastro-**
712   **oesophageal junction cancer refractory to, or intolerant of, at least two**
713   **previous chemotherapy regimens (ONO-4538-12, ATTRACTION-2): a**
714   **randomised, double-blind, placebo-controlled, phase 3 trial.** *Lancet* 2017,
715   **390:**2461-2471.
716 60. Devarajan K: **Non-negative matrix factorization: an analytical and interpretive**
717   **tool in computational biology.** *PLoS Comput Biol* 2008, **4:**e1000029.

718   61.   Pehkonen P, Wong G, Toronen P: **Theme discovery from gene lists for**
719   **identification and viewing of multiple functional groups.** *BMC Bioinformatics*
720   2005, **6:**162.
721   62.   Zhou YJ, Zhu GQ, Lu XF, Zheng KI, Wang QW, Chen JN, Zhang QW, Yan FR, Li
722   XB: **Identification and validation of tumour microenvironment-based immune**
723   **molecular subgroups for gastric cancer: immunotherapeutic implications.**
724   *Cancer Immunol Immunother* 2020, **69:**1057-1069.
725   63.   Chen YP, Wang YQ, Lv JW, Li YQ, Chua MLK, Le QT, Lee N, Colevas AD, Seiwert
726   T, Hayes DN, et al: **Identification and validation of novel microenvironment-**
727   **based immune molecular subgroups of head and neck squamous cell**
728   **carcinoma: implications for immunotherapy.** *Ann Oncol* 2019, **30:**68-75.
729   64.   Sia D, Jiao Y, Martinez-Quetglas I, Kuchuk O, Villacorta-Martin C, Castro de Moura
730   M, Putra J, Camprecios G, Bassaganyas L, Akers N, et al: **Identification of an**
731   **Immune-specific Class of Hepatocellular Carcinoma, Based on Molecular**
732   **Features.** *Gastroenterology* 2017, **153:**812-826.
733   65.   Bald T, Landsberg J, Lopez-Ramos D, Renn M, Glodde N, Jansen P, Gaffal E,
734   Steitz J, Tolba R, Kalinke U, et al: **Immune cell-poor melanomas benefit from**
735   **PD-1 blockade after targeted type I IFN activation.** *Cancer Discov* 2014, **4:**674-
736   687.
737   66.   Rooney MS, Shukla SA, Wu CJ, Getz G, Hacohen N: **Molecular and genetic**
738   **properties of tumors associated with local immune cytolytic activity.** *Cell*
739   2015, **160:**48-61.
740   67.   Perou CM, Sorlie T, Eisen MB, van de Rijn M, Jeffrey SS, Rees CA, Pollack JR,
741   Ross DT, Johnsen H, Akslen LA, et al: **Molecular portraits of human breast**
742   **tumours.** *Nature* 2000, **406:**747-752.
743   68.   Ellis MJ, Suman VJ, Hoog J, Lin L, Snider J, Prat A, Parker JS, Luo J, DeSchryver
744   K, Allred DC, et al: **Randomized phase II neoadjuvant comparison between**
745   **letrozole, anastrozole, and exemestane for postmenopausal women with**
746   **estrogen receptor-rich stage 2 to 3 breast cancer: clinical and biomarker**
747   **outcomes and predictive value of the baseline PAM50-based intrinsic**
748   **subtype--ACOSOG Z1031.** *J Clin Oncol* 2011, **29:**2342-2349.
749   69.   Choi W, Porten S, Kim S, Willis D, Plimack ER, Hoffman-Censits J, Roth B, Cheng
750   T, Tran M, Lee IL, et al: **Identification of distinct basal and luminal subtypes**
751   **of muscle-invasive bladder cancer with different sensitivities to frontline**
752   **chemotherapy.** *Cancer Cell* 2014, **25:**152-165.
753   70.   Chia SK, Bramwell VH, Tu D, Shepherd LE, Jiang S, Vickery T, Mardis E, Leung
754   S, Ung K, Pritchard KI, et al: **A 50-gene intrinsic subtype classifier for**
755   **prognosis and prediction of benefit from adjuvant tamoxifen.** *Clin Cancer Res*
756   2012, **18:**4465-4472.
757   71.   Zhu B, Tse LA, Wang D, Koka H, Zhang T, Abubakar M, Lee P, Wang F, Wu C,
758   Tsang KH, et al: **Immune gene expression profiling reveals heterogeneity in**
759   **luminal breast tumors.** *Breast Cancer Res* 2019, **21:**147.
760   72.   Poudel P, Nyamundanda G, Patil Y, Cheang MCU, Sadanandam A:
761   **Heterocellular gene signatures reveal luminal-A breast cancer heterogeneity**
762   **and differential therapeutic responses.** *NPJ Breast Cancer* 2019, **5:**21.
763   73.   Derhovanessian E, Adams V, Hahnel K, Groeger A, Pandha H, Ward S, Pawelec
764   G: **Pretreatment frequency of circulating IL-17+ CD4+ T-cells, but not Tregs,**
765   **correlates with clinical response to whole-cell vaccination in prostate cancer**
766   **patients.** *Int J Cancer* 2009, **125:**1372-1379.
767   74.   Budczies J, Denkert C, Gyorffy B, Schirmacher P, Stenzinger A: **Chromosome 9p**
768   **copy number gains involving PD-L1 are associated with a specific**

769   **proliferation and immune-modulating gene expression program active**
770   **across major cancer types.** *BMC Med Genomics* 2017, **10:**74.

771 75. Van Allen EM, Miao D, Schilling B, Shukla SA, Blank C, Zimmer L, Sucker A, Hillen
772   U, Foppen MHG, Goldinger SM, et al: **Genomic correlates of response to CTLA-**
773   **4 blockade in metastatic melanoma.** *Science* 2015, **350:**207-211.

774 76. Rizvi NA, Hellmann MD, Snyder A, Kvistborg P, Makarov V, Havel JJ, Lee W, Yuan
775   J, Wong P, Ho TS, et al: **Cancer immunology. Mutational landscape**
776   **determines sensitivity to PD-1 blockade in non-small cell lung cancer.**
777   *Science* 2015, **348:**124-128.

778 77. Subudhi SK, Vence L, Zhao H, Blando J, Yadav SS, Xiong Q, Reuben A, Aparicio
779   A, Corn PG, Chapin BF, et al: **Neoantigen responses, immune correlates, and**
780   **favorable outcomes after ipilimumab treatment of patients with prostate**
781   **cancer.** *Sci Transl Med* 2020, **12**.

782 78. Jiang Z, Liu Z, Li M, Chen C, Wang X: **Immunogenomics Analysis Reveals that**
783   **TP53 Mutations Inhibit Tumor Immunity in Gastric Cancer.** *Transl Oncol* 2018,
784   **11:**1171-1187.

785 79. Jennifer WC, Nhu, Thi Nho, Chaejin, Kim, Zhengjia, Chen, Shiyong, Li, Charles,
786   Hill, Suresh, S. Ramalingam, Gabriel, Sica, Taofeek, Kunle Owonikoko: **Impact of**
787   **TP53 mutations on efficacy of PD-1 targeted immunotherapy in non-small**
788   **cell lung cancer (NSCLC).** *Journal of Clinical Oncology* 2018, **36:**e21090.

789 80. Zhang J, Bu X, Wang H, Zhu Y, Geng Y, Nihira NT, Tan Y, Ci Y, Wu F, Dai X, et
790   al: **Cyclin D-CDK4 kinase destabilizes PD-L1 via cullin 3-SPOP to control**
791   **cancer immune surveillance.** *Nature* 2018, **553:**91-95.

792 81. Knudson KM, Hicks KC, Luo X, Chen JQ, Schlom J, Gameiro SR: **M7824, a novel**
793   **bifunctional anti-PD-L1/TGFbeta Trap fusion protein, promotes anti-tumor**
794   **efficacy as monotherapy and in combination with vaccine.** *Oncoimmunology*
795   2018, **7:**e1426519.

796 82. Wolchok JD, Kluger H, Callahan MK, Postow MA, Rizvi NA, Lesokhin AM, Segal
797   NH, Ariyan CE, Gordon RA, Reed K, et al: **Nivolumab plus ipilimumab in**
798   **advanced melanoma.** *N Engl J Med* 2013, **369:**122-133.

799 83. Motzer RJ, Rini BI, McDermott DF, Aren Frontera O, Hammers HJ, Carducci MA,
800   Salman P, Escudier B, Beuselinck B, Amin A, et al: **Nivolumab plus ipilimumab**
801   **versus sunitinib in first-line treatment for advanced renal cell carcinoma:**
802   **extended follow-up of efficacy and safety results from a randomised,**
803   **controlled, phase 3 trial.** *Lancet Oncol* 2019, **20:**1370-1385.

804 84. Hellmann MD, Paz-Ares L, Bernabe Caro R, Zurawski B, Kim SW, Carcsreny
805   Costa E, Park K, Alexandru A, Lupinacci L, de la Mora Jimenez E, et al:
806   **Nivolumab plus Ipilimumab in Advanced Non-Small-Cell Lung Cancer.** *N Engl*
807   *J Med* 2019, **381:**2020-2031.

808

809

810

811

812 **Figure Legends**

813 **Figure 1. Flow chart of the current study.** A total of 1,557 prostate cancer patients were

814 analyzed, and the immunophenotypes were identified in 495 patients from the TCGA-

815 PRAD cohort and validated in the GSE70770, GSE116918, GSE79021, MSKCC, and

816 AHMU-PC cohorts. TCGA-PRAD, The Cancer Genome Atlas-prostate adenocarcinoma;

817 MSKCC, Memorial Sloan-Kettering Cancer Center.

818 **Figure 2. Identification of the immune-related clustering factor by non-negative**

819 **matrix factorization (NMF) analysis.** (A) 11 clustering factors obtained from NMF

820 analysis, with the second factor enriched the most patients with high immune enrichment

821 scores. (B) The immune and non-immune class were adjusted by the multidimensional

822 scaling (MDS) random forest method, with the gene expression matrix of the top 150

823 exemplar genes. (C) Heatmap showing the distribution of patients in different NMF factors,

824 immune factor weight, exemplar gene clustering, IES, and final immune class. (D) GSEA

825 results showing the activated signaling pathways in the immune class.

826 **Figure 3. Identification of the immunophenotypes among the TCGA-PRAD cohort.**

827 Consensus-clustered heatmap by the exemplar genes of NMF selected immune factor

828 and refined by MDS random forest to define the immune class (200/495, 40.4%, sky-blue

829 bar); nearest Template Prediction (NTP) using a signature capturing activated stroma

830 identified two distinct immune response subtypes: immune-suppressed (126/495, 25.5%;

831 light-green bar) and immune activated (74/495, 14.9%; red bar); in the heat map, high and

832 low single-sample gene set enrichment scores are represented in red and blue,

833 respectively. Positive prediction of activated stroma signature as per NTP is indicated in

834 brown and its absence is in grey. TCGA-PRAD, The Cancer Genome Atlas-prostate

835 adenocarcinoma; CYT, cytolytic activity score; TITR, tumor-infiltrating Tregs; MDSC,

30

836 myeloid-derived suppressor cell; TLS, tertiary lymphoid structure; C-ECM, cancer-

837 associated extracellular matrix.

838 **Figure 4. Associations of immune class with tumor-infiltrating lymphocytes, copy**

839 **number alterations, gene mutation, neoantigens, tumor stemness, and PD-L1**

840 **expression.** (A) Arm-level copy number amplification and deletion; (B) Focal-level copy

841 number amplification and deletion; (C) Tumor mutant burden difference; (D) Differentially

842 mutated genes among three immune subgroups (some patients without gene mutations

843 in non-immune class did not show); (E) Neoantigens difference; (F) Tumor-infiltrating

844 lymphocytes difference; (G) PD-L1 expression difference; (H) Tumor stemness difference

845 represented by the mRNAsi.

846 **Figure 5. Successful validation of the immunophenotypes among three external**

847 **Gene Expression Omnibus (GEO) cohorts.** Consensus-clustered heatmap by the top

848 150 differentially expressed genes (DEGs) among immune and non-immune classes in

849 the training cohort were conducted to generate the immune and non-immune classes in

850 the validation cohort, and further divided into suppressed and activation classes by

851 activated stroma signature; In the heat map, high and low single-sample gene set

852 enrichment scores are represented in red and blue, respectively. Positive prediction of

853 activated stroma signature as per NTP is indicated in brown and its absence is in grey.

854 CYT, cytolytic activity score; TITR, tumor-infiltrating Tregs; MDSC, myeloid-derived

855 suppressor cell; TLS, tertiary lymphoid structure; C-ECM, cancer-associated extracellular

856 matrix.

857 **Figure 6. Immunophenotypes associated with the different recurrence-free survival**

858 **outcomes of prostate cancer patients.** (A) Different recurrence-free survival in three

859 immunophenotypes among patients less or equal to 60 years old in TCGA-PRAD cohort;

31

860   (B) different recurrence-free survival in three immunophenotypes in GSE70770 cohort; (C)

861   different recurrence-free survival in three immunophenotypes in GSE116918 cohort; (D)

862   different recurrence-free survival in three immunophenotypes in MSKCC cohort. TCGA,

863   The Cancer Genome Atlas-prostate adenocarcinoma; MSKCC, Memorial Sloan-Kettering

864   Cancer Center.

865   **Figure 7. Successful validation of the immunophenotypes in the AHMU-PC cohort.**

866   (A) Heatmap showing the different enrichment of characteristic signatures among immune

867   activated, immune suppressed and non-immune groups; (B) Kaplan-Meier plot showing

868   the recurrence-free survival outcome in three immunophenotypes; (C) Subclass mapping

869   (SubMap) analysis manifested that patients with immune activated subtype were more

870   likely to respond to anti–PD-1/PD-L1 treatment (Bonferroni corrected P-value = 0.0399).

871   **Supplementary Figure 1. Pathway enrichment of the top 150 exemplar genes.** (A)

872   The function enrichment of the top 150 exemplar genes in Gene Ontology (GO) Biological

873   Process (BP), Molecular Function (MF), and Cellular Component (CC). (B) The enriched

874   genes in T cell activation, Leukocyte migration, and Lymphocyte differentiation pathways.

875   The top-weighted genes in each pathway were marked with red color.

876   **Supplementary Figure 2. The association between the infiltration of immunocytes**

877   **and the top 5 exemplar genes of immune factor.**

878   **Supplementary Figure 3. The different expressions of stromal markers and**

879   **infiltration of Th17 cells in immune activated and suppressed classes.**

880   **Supplementary Figure 4. The association between copy number variation of**

881   **immune checkpoints and immunocyte infiltration.**

882 **Supplementary Figure 5. The association between the infiltration of immunocytes**

883 **and the top 5 differentially expressed genes among immune and non-immune**

884 **classes.**

885 **Supplementary Figure 6. Successful validation of the immunophenotypes among**

886 **the GSE79021 cohort.** Consensus-clustered heatmap by the top 150 differentially

887 expressed genes among immune and non-immune classes in the training cohort were

888 conducted to generate the immune and non-immune classes in the validation cohort, and

889 further divided into suppressed and activation classes by activated stroma signature; In

890 the heat map, high and low single-sample gene set enrichment scores are represented in

891 red and blue, respectively. Positive prediction of activated stroma signature as per NTP is

892 indicated in brown and its absence is in grey. CYT, cytolytic activity score; TITR, tumor-

893 infiltrating Tregs; MDSC, myeloid-derived suppressor cell; TLS, tertiary lymphoid structure;

894 C-ECM, cancer-associated extracellular matrix.

895 **Supplementary Figure 7. The distribution of clinicopathological features among**

896 **three immunophenotypes in four cohorts.** Immune sup: Immune suppressed subtype;

897 Immune act: Immune activated subtype.

898 **Supplementary Figure 8. Association of the three immunophenotypes with the six**

899 **pan-cancer immune molecular subgroups.**

900 **Supplementary Figure 9. Association of the three immunophenotypes with the**

901 **PAM50 molecular subtypes.**

902 **Supplementary Figure 10. Genetic similarity between patients of Immune Class and**

903 **patients with melanoma responsive to anti–PD-1/anti–CTLA-4 immunotherapy.**

904 Subclass mapping (SubMap) analysis manifested that patients with immune activated

33

905   subtype were more likely to respond to anti–PD-1 treatment (Bonferroni corrected P-value

906   = 0.0079).

907   **Supplementary Figure 11. The distribution of the Gleason score and pathological T**

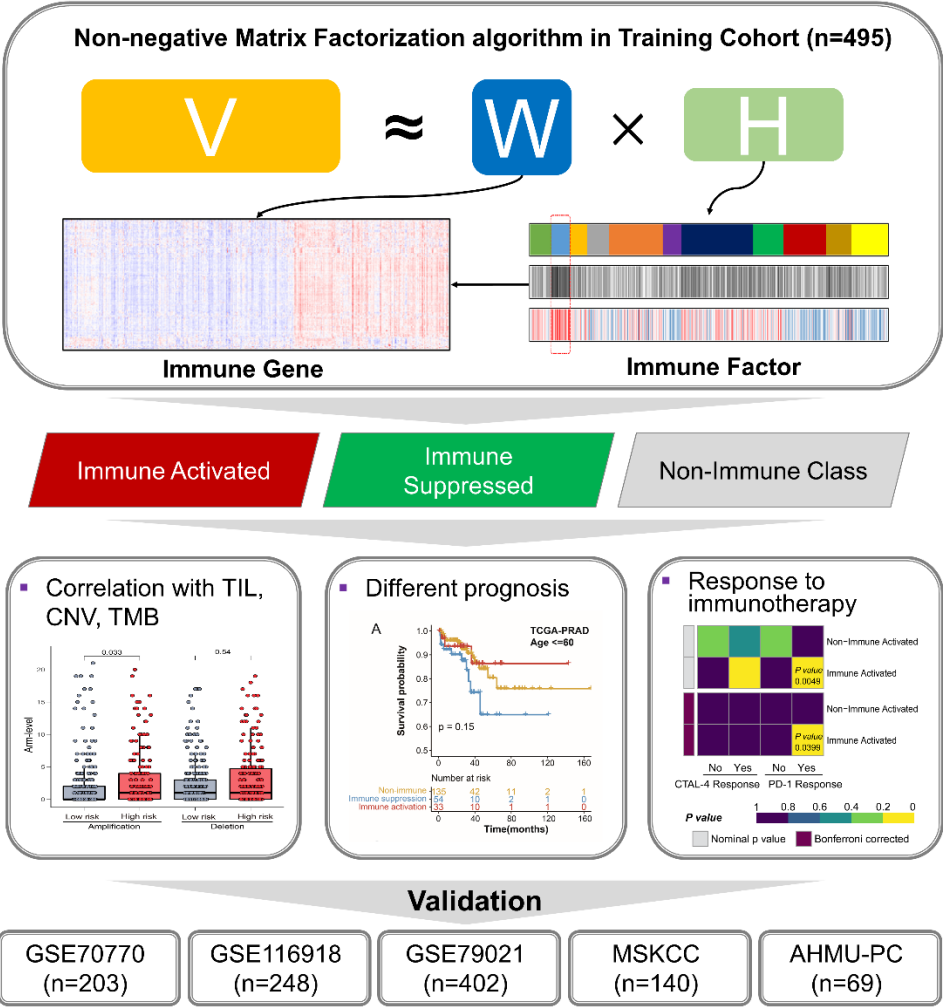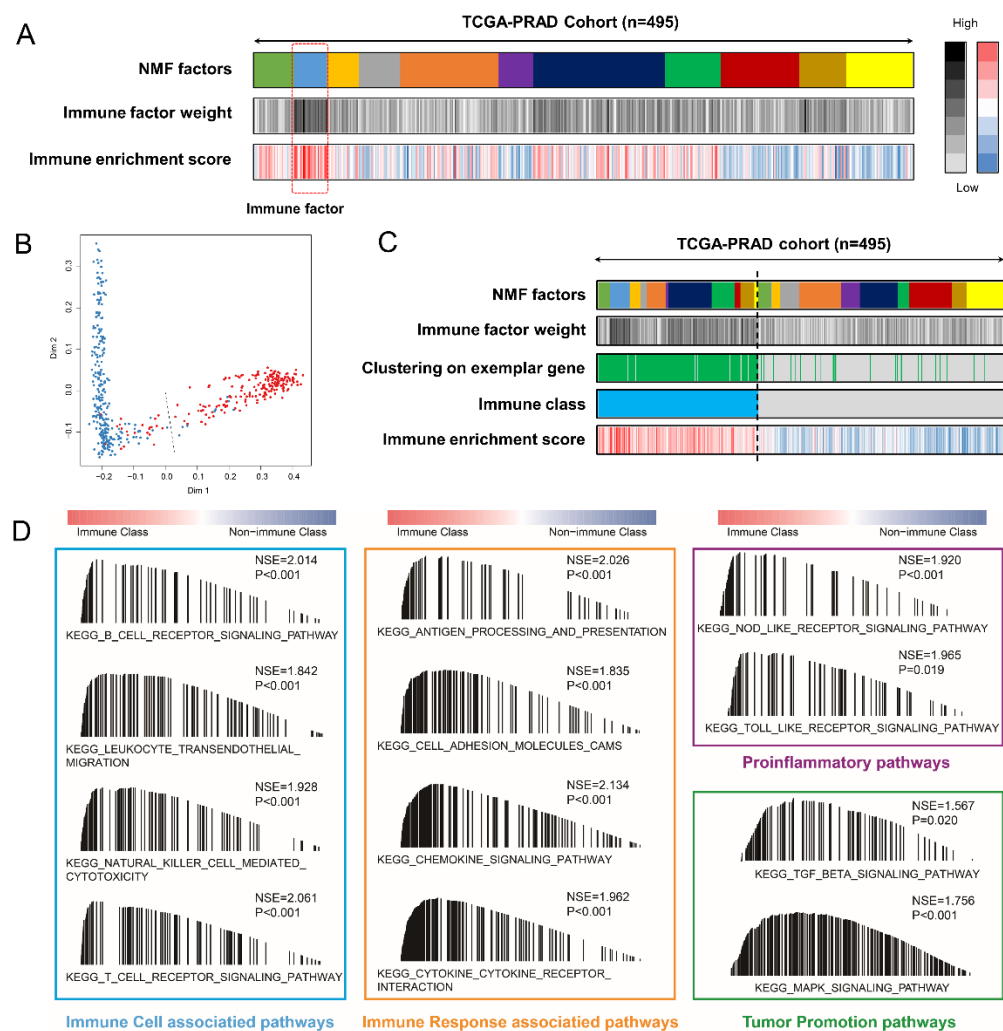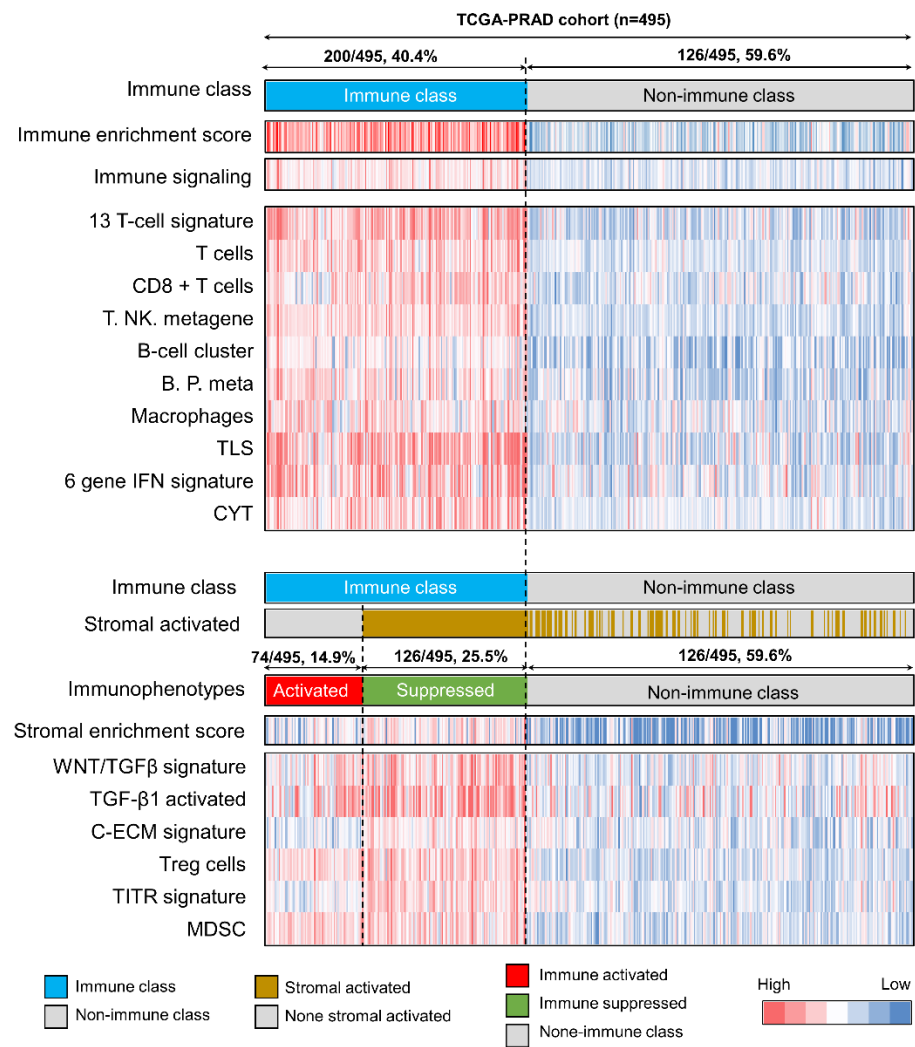908   **stage among three immunophenotypes in the AHMU-PC cohort.**

909

910

911

912

913

914

915
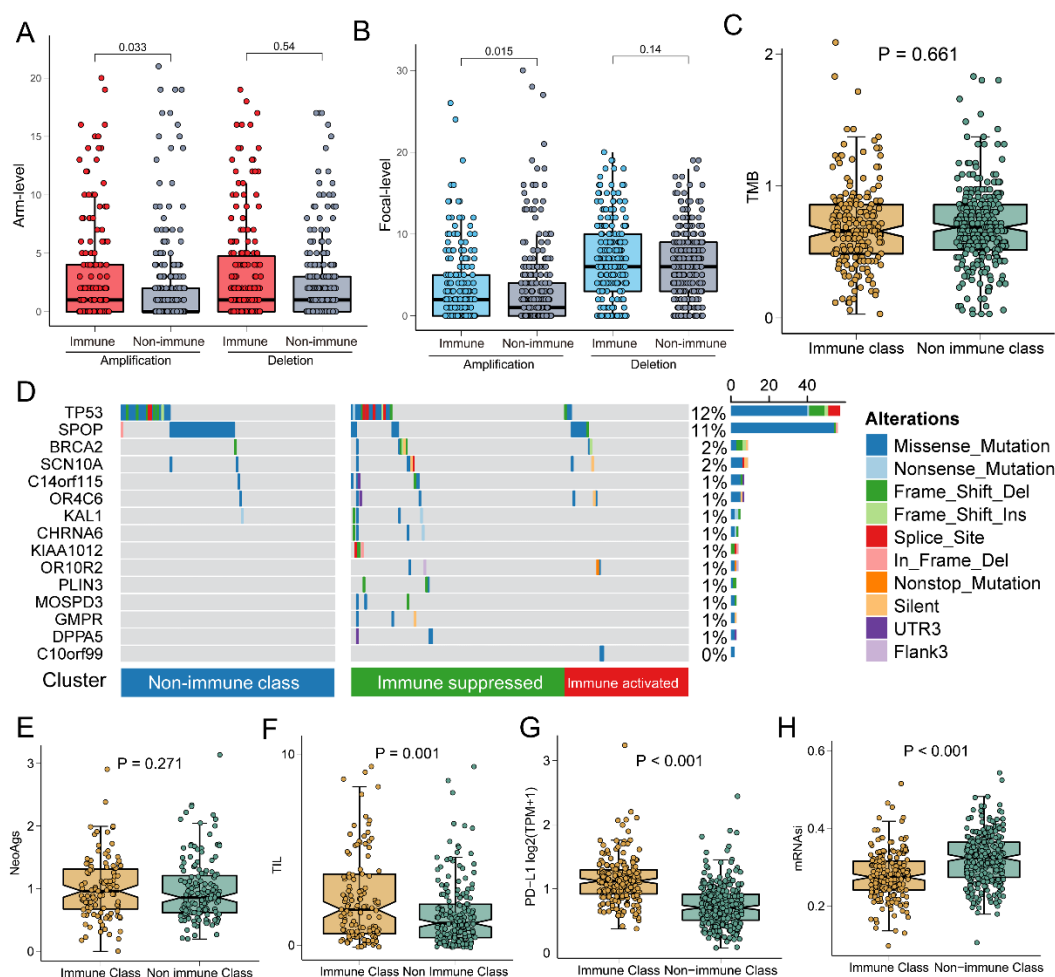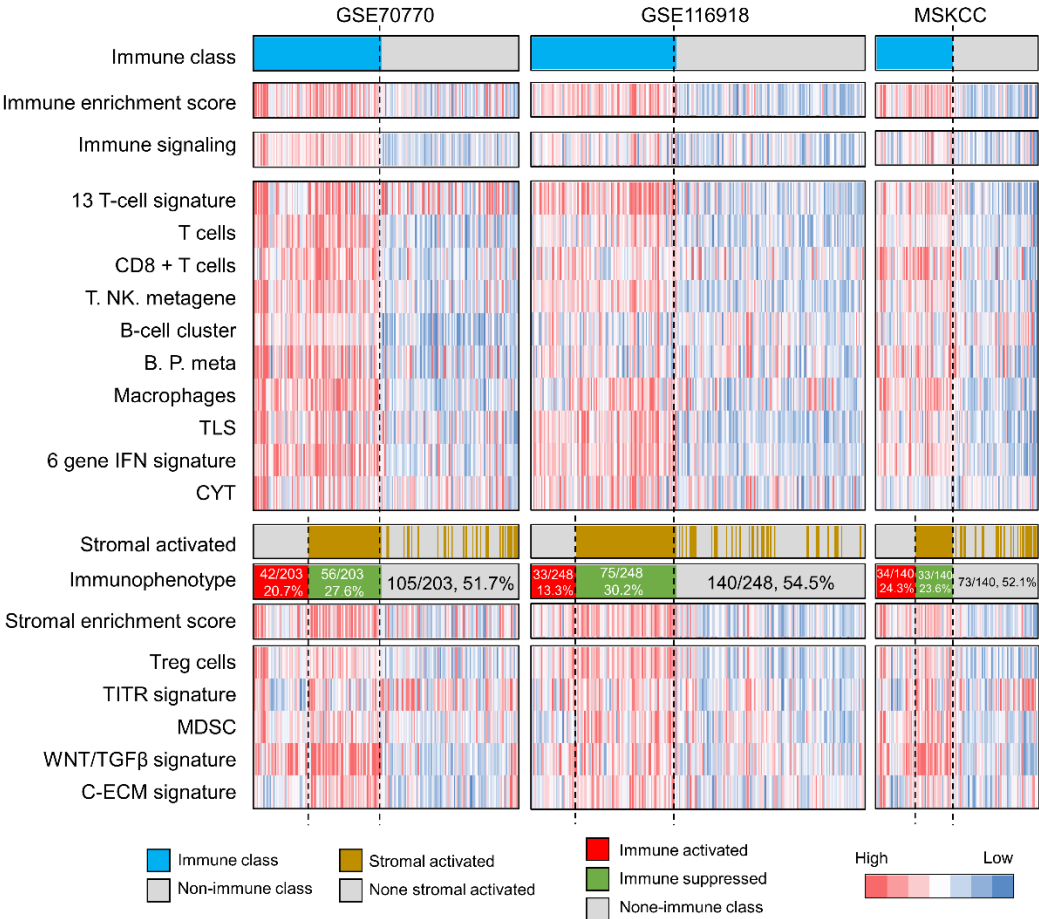
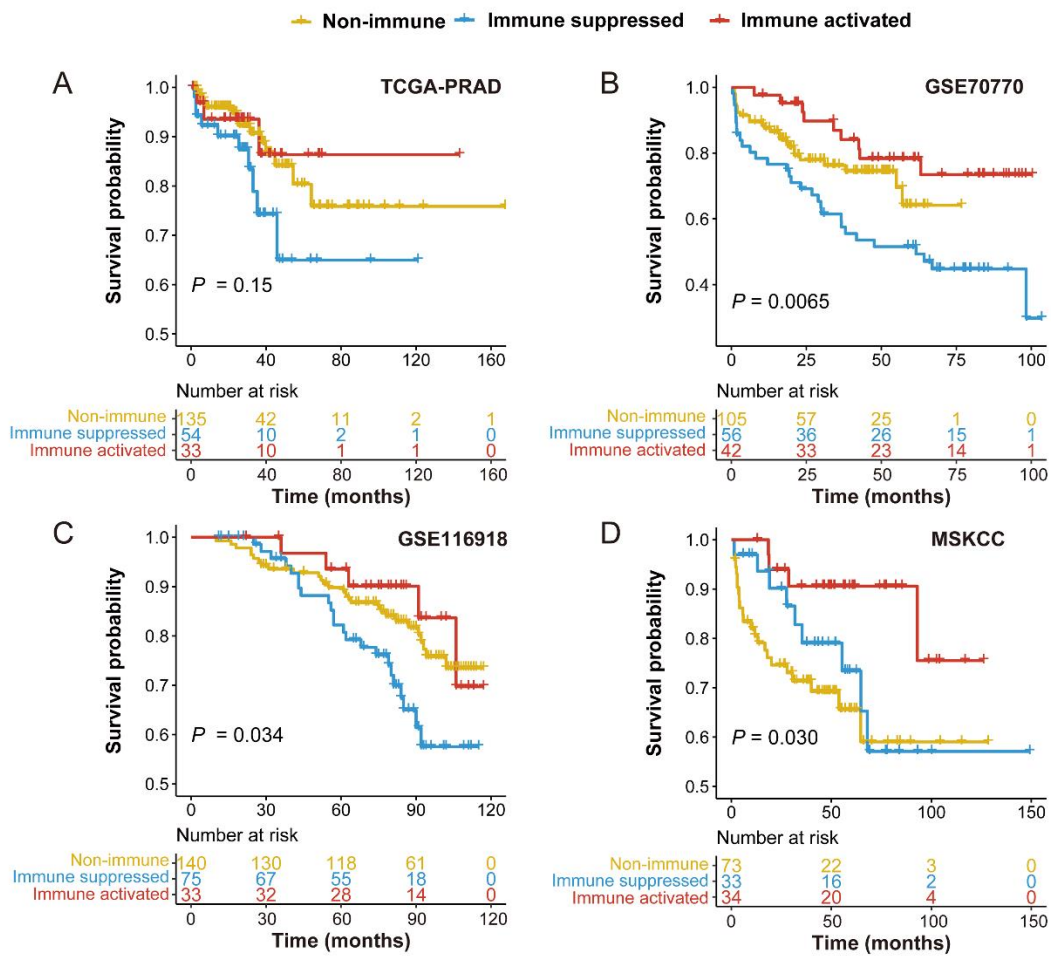916

917

918

919

920

921

922

Figure 1

923

Figure 2

924

Figure 3

925

926 Figure 4

Figure 5

927

Figure 6

928

Figure 7

929